Erschienen in: Optics Express ; 23 (2015), 7. - S. 8901-8909

Diode-pumped continuous-wave and femtosecond Cr:LiCAF lasers with high average power in the near infrared, visible and near ultraviolet

Umit Demirbas,[1,2,*] Ilyes Baali,[2] Durmus Alp Emre Acar,[2] and Alfred Leitenstorfer[1]

[1]*Department of Physics and Center for Applied Photonics, University of Konstanz, D-78464 Konstanz, Germany*
[2]*Laser Technology Laboratory, Department of Electrical and Electronics Engineering, International Antalya University, 07190 Antalya, Turkey*
[*]*umit79@alum.mit.edu*

Abstract: We demonstrate continuous-wave (cw), cw frequency-doubled, cw mode-locked and Q-switched mode-locked operation of multimode diode-pumped Cr:LiCAF lasers with record average powers. Up to 2.54 W of cw output is obtained around 805 nm at an absorbed pump power of 5.5 W. Using intracavity frequency doubling with a BBO crystal, 0.9 W are generated around 402 nm, corresponding to an optical-to-optical conversion efficiency of 12%. With an intracavity birefringent tuning plate, the fundamental and frequency-doubled laser output is tuned continuously in a broad wavelength range from 745 nm to 885 nm and from 375 to 440 nm, respectively. A saturable Bragg reflector is used to initiate and sustain mode locking. In the cw mode-locked regime, the Cr:LiCAF laser produces 105-fs long pulses near 810 nm with an average power of 0.75 W. The repetition rate is 96.4 MHz, resulting in pulse energies of 7.7 nJ and peak powers of 65 kW. In Q-switched mode-locked operation, pulses with energies above 150 nJ are generated.

OCIS codes: (140.3600) Lasers, tunable; (140.4050) Mode-locked lasers; (140.3580) Lasers, solid-state; (140.3480) Lasers, diode pumped; (140.3515) Lasers, frequency doubled.

References and links

1. S. A. Payne, L. L. Chase, L. K. Smith, W. L. Kway, and H. W. Newkirk, "Laser performance of $LiSAlF_6:Cr^{3+}$," J. Appl. Phys. **66**(3), 1051–1056 (1989).
2. S. A. Payne, L. L. Chase, H. W. Newkirk, L. K. Smith, and W. F. Krupke, "$LiCaAlF_6:Cr^{3+}$ a promising new solid-state laser material," IEEE J. Quantum Electron. **24**(11), 2243–2252 (1988).
3. L. K. Smith, S. A. Payne, W. L. Kway, L. L. Chase, and B. H. T. Chai, "Investigation of the laser properties of Cr^{3+}:$LiSrGaF_6$," IEEE J. Quantum Electron. **28**(11), 2612–2618 (1992).
4. I. T. Sorokina, E. Sorokin, E. Wintner, A. Cassanho, H. P. Jenssen, and R. Szipöcs, "14-fs pulse generation in Kerr-lens mode-locked prismless Cr:LiSGaF and Cr:LiSAF lasers: observation of pulse self-frequency shift," Opt. Lett. **22**(22), 1716–1718 (1997).
5. S. Uemura and K. Torizuka, "Generation of 10 fs pulses from a diode-pumped Kerr-lens mode-locked Cr: LiSAF laser," Jpn. J. Appl. Phys. **39**(Part 1, No. 6A), 3472–3473 (2000).
6. P. C. Wagenblast, U. Morgner, F. Grawert, T. R. Schibli, F. X. Kãârtner, V. Scheuer, G. Angelow, and M. J. Lederer, "Generation of sub-10-fs pulses from a Kerr-lens mode-locked Cr^{3+}:LiCAF laser oscillator by use of third-order dispersion-compensating double-chirped mirrors," Opt. Lett. **27**(19), 1726–1728 (2002).
7. U. Demirbas, S. Eggert, and A. Leitenstorfer, "Compact and efficient Cr:LiSAF lasers pumped by one single-spatial-mode diode: a minimal cost approach," J. Opt. Soc. Am. B **29**(8), 1894–1903 (2012).
8. R. Scheps, J. F. Myers, H. B. Serreze, A. Rosenberg, R. C. Morris, and M. Long, "Diode-pumped $Cr:LiSrAlF_6$ laser," Opt. Lett. **16**(11), 820–822 (1991).
9. S. Tsuda, W. H. Knox, and S. T. Cundiff, "High efficiency diode pumping of a saturable Bragg reflector-mode-locked Cr:LiSAF femtosecond laser," Appl. Phys. Lett. **69**(11), 1538–1540 (1996).
10. G. J. Valentine, J. M. Hopkins, P. Loza-Alvarez, G. T. Kennedy, W. Sibbett, D. Burns, and A. Valster, "Ultralow-pump-threshold, femtosecond Cr^{3+}:$LiSrAlF_6$ laser pumped by a single narrow-stripe AlGaInP laser diode," Opt. Lett. **22**(21), 1639–1641 (1997).
11. B. Agate, B. Stormont, A. J. Kemp, C. T. A. Brown, U. Keller, and W. Sibbett, "Simplified cavity designs for efficient and compact femtosecond Cr:LiSAF lasers," Opt. Commun. **205**(1-3), 207–213 (2002).

#233863 - $15.00 USD Received 3 Feb 2015; revised 10 Mar 2015; accepted 10 Mar 2015; published 30 Mar 2015

12. D. Kopf, K. J. Weingarten, G. Zhang, M. Moser, M. A. Emanuel, R. J. Beach, J. A. Skidmore, and U. Keller, "High-average-power diode-pumped femtosecond Cr:LiSAF lasers," Appl. Phys. B **65**(2), 235–243 (1997).
13. A. Isemann and C. Fallnich, "High-power colquiriite lasers with high slope efficiencies pumped by broad-area laser diodes," Opt. Express **11**(3), 259–264 (2003).
14. A. Dergachev, J. H. Flint, Y. Isyanova, B. Pati, E. V. Slobodtchikov, K. F. Wall, and P. F. Moulton, "Review of multipass slab laser systems," IEEE J. Sel. Top. Quantum Electron. **13**(3), 647–660 (2007).
15. U. Demirbas, R. Uecker, D. Klimm, B. Sumpf, and G. Erbert, "Intra-cavity frequency-doubled Cr:LiCAF laser with 265 mW continuous-wave blue (395-405 nm) output," Opt. Commun. **320**, 38–42 (2014).
16. M. Stalder, M. Bass, and B. H. T. Chai, "Thermal quenching of fluoresence in chromium-doped fluoride laser crystals," J. Opt. Soc. Am. B **9**(12), 2271–2273 (1992).
17. J. K. Jabczynski, W. Zendzian, Z. Mierczyk, and Z. Frukacz, "Chromium-doped LiCAF laser passively Q switched with a V^{3+}:YAG crystal," Appl. Opt. **40**(36), 6638–6645 (2001).
18. D. Klimm and P. Reiche, "Ternary colquiriite type fluorides as laser hosts," Cryst. Res. Technol. **34**(2), 145–152 (1999).
19. D. Klimm, R. Uecker, and P. Reiche, "Melting behavior and growth of colquiriite laser crystals," Cryst. Res. Technol. **40**(4-5), 352–358 (2005).
20. U. Demirbas, A. Sennaroglu, F. X. Kartner, and J. G. Fujimoto, "Comparative investigation of diode pumping for continuous-wave and mode-locked Cr3+: LiCAF lasers," J. Opt. Soc. Am. B **26**(1), 64–79 (2009).
21. U. Demirbas, M. Schmalz, B. Sumpf, G. Erbert, G. S. Petrich, L. A. Kolodziejski, J. G. Fujimoto, F. X. Kärtner, and A. Leitenstorfer, "Femtosecond Cr:LiSAF and Cr:LiCAF lasers pumped by tapered diode lasers," Opt. Express **19**(21), 20444–20461 (2011).
22. U. O. Farrukh, "Estimating stress and strain in end-pumped laser crystals: The case of Cr:LiCAF rod," Modeling and Simulation of Higher-Power Laser Systems Iv **2989**, 48–56 (1997).
23. B. W. Woods, S. A. Payne, J. E. Marion, R. S. Hughes, and L. E. Davis, "Thermomechanical and thermooptic properties of the $LiCaAlF_6$-Cr^{3+} laser material," J. Opt. Soc. Am. B **8**, 970–977 (1991).
24. L. J. Atherton, S. A. Payne, and C. D. Brandle, "Oxide and fluoride laser crystals," Annu. Rev. Mater. Sci. **23**(1), 453–502 (1993).
25. S. Makio, M. Sato, and T. Sasaki, "High-power, continuous-wave and blue light generation by intracavity frequency doubling of a Cr:$LiSrAlF_6$ Laser," Jpn. J. Appl. Phys. **40**(Part 1, No. 4A), 2278–2281 (2001).
26. R. G. Smith, "Theory of intracavity optical second-harmonic generation," IEEE J. Quantum Electron. **6**(4), 215–223 (1970).
27. H. Maestre, A. J. Torregrosa, and J. Capmany, "Intracavity Cr3+:LiCAF + PPSLT optical parametric oscillator with self-injection-locked pump wave," Laser Phys. Lett. **10**(3), 035806 (2013).
28. A. Sennaroglu, A. M. Kowalevicz, A. Zare, and J. G. Fujimoto, "General design rules for multi-pass cavity lasers in ultrashort pulse generation," in Conference on Lasers and Electro-Optics (CLEO) (IEEE, 2004), 3 pp. vol.1.
29. S. Sakadzić, U. Demirbas, T. R. Mempel, A. Moore, S. Ruvinskaya, D. A. Boas, A. Sennaroglu, F. X. Kaertner, and J. G. Fujimoto, "Multi-photon microscopy with a low-cost and highly efficient Cr:LiCAF laser," Opt. Express **16**(25), 20848–20863 (2008).
30. D. Kobat, M. E. Durst, N. Nishimura, A. W. Wong, C. B. Schaffer, and C. Xu, "Deep tissue multiphoton microscopy using longer wavelength excitation," Opt. Express **17**(16), 13354–13364 (2009).
31. A. M. Kowalevicz, V. Sharma, E. P. Ippen, J. G. Fujimoto, and K. Minoshima, "Three-dimensional photonic devices fabricated in glass by use of a femtosecond laser oscillator," Opt. Lett. **30**(9), 1060–1062 (2005).

1. Introduction

Cr^{3+}-doped colquiriites (Cr^{+3}:$LiSrAlF_6$ [1], Cr^{+3}:$LiCaAlF_6$ [2] and Cr^{+3}:$LiSrGaF_6$ [3]) offer broad emission bands in the near infrared that allow generation of sub-10-fs light pulses via mode-locking [4–6] and widely tunable laser operation in the wavelength range between 700 nm and 1100 nm [7]. Via second-harmonic generation, tunability may be extended into the ultraviolet, blue and green regions of the spectrum from 350 nm to 550 nm. Cr:colquiriites also exhibit absorption bands between 600 nm and 700 nm that enable efficient pumping with low-cost laser diodes [8–11]. They further possess low passive losses, low quantum defect, a large florescence lifetime and emission cross section product value, and high intrinsic slope efficiencies. These properties facilitate construction of compact and efficient cw and cw mode-locked Cr:colquiriite lasers that can replace more costly Ti:sapphire-based systems in selected applications.

On the other hand, power scaling of Cr:colquiriite lasers has been challenging. First of all, the host thermal conductivities are almost an order of magnitude lower as compared to Ti:sapphire. In addition, relatively strong excited-state absorption and Auger upconversion occur in Cr:colquiriites, resulting in considerable thermal load on the gain crystals. Furthermore, the output beams from high-power pump diodes are quite structured (M^2 of 10 or worse), creating additional thermal load due to imperfect mode-matching. Lastly, Cr:colquiriites also suffer from a relatively low limit for thermal fracture which causes

#233863 - $15.00 USD Received 3 Feb 2015; revised 10 Mar 2015; accepted 10 Mar 2015; published 30 Mar 2015

damage of the laser crystal at high pump powers. These drawbacks considerably limit the output performance available from Cr:colquiriite lasers [12–14], considerably restricting their functionality.

The highest cw output power reported from Cr:colquiriites to date is 3 W [14]. For this result, Dergachev et al. used a multi-pass slab laser geometry and a 27 mm long and 1 mm thick Cr:LiSAF crystal that is pumped by two 15-W diode bars. In this way, an optical-to-optical conversion efficiency of 10% is achieved. In another work, Kopf et al. employed a carefully designed Cr:LiSAF laser with cylindrical cavity mirrors and a very thin crystal with an optimized cooling geometry to minimize thermal effects [12]. A 15-W laser diode array pumped a 1-mm thick Cr:LiSAF crystal (0.8% chromium doping), which produced up to 1.54 W of cw output power, also at a conversion efficiency around 10%. This Cr:LiSAF system also produced 110-fs long pulses with 500 mW of average power. In terms of frequency-doubled output, the highest cw power obtained previously is 265 mW [15].

In this work, we have chosen to work with Cr:LiCAF since it is the most suitable candidate for high-power applications. Among Cr:colquiriites, Cr:LiCAF has the highest thermal conductivity and maximum thermal quenching temperature combined with minimum quantum defect, excited-state absorption and upconversion rate [12, 16, 17]. Despite these facts, earlier studies with Cr:colquiriites mostly focused on Cr:LiSAF due to its broader gain bandwidth, slightly higher gain and availability of high-quality crystals with low passive losses in the order of 0.2% cm^{-1}. On the other hand, earlier Cr:LiCAF samples had high extrinsic losses around 2% cm^{-1} due to nanoscale precipitates generated during the growth process [18]. With improvement in crystal quality over the last decade [19], Cr:LiCAF has recently started to attract the desired attention. The highest output powers reported from Cr:LiCAF are 1 W in cw operation [20] and 415 mW under cw mode locking [21]. Comparing with the performance of Cr:LiSAF systems and taking into account the superior physical properties of Cr:LiCAF, the power levels obtained with this material indicate that the intrinsic limits of its technology have not yet been investigated.

The objective of this paper is to demonstrate feasibility of further power scaling with Cr:LiCAF as a gain medium and to check out the limitations set by the material itself. Four broad-area laser diodes constitute the pump source providing a total power of 7.2 W. In continuous-wave lasing experiments, up to 2.54-W of near-infrared output was obtained around 800 nm at an absorbed pump power of 5.5 W and using a 2% output coupler. The threshold and slope efficiency were 180 mW and 49%, respectively, resulting in an optical-to-optical conversion efficiency of 35%. Intracavity frequency doubling with a beta-barium borate (BBO) crystal enabled generation of cw blue powers up to 900 mW at an optical-to-optical conversion efficiency of 12.5%. Using an intracavity birefringent plate, the fundamental and frequency-doubled laser output could be tuned continuously from 745 nm to 885 nm and from 375 nm to 440 nm, respectively. In the cw mode-locked regime, the Cr:LiCAF laser produced 105-fs long pulses near 810 nm with an average power of 0.75 W. The repetition rate was 96.4 MHz, corresponding to pulse energies of 7.7 nJ and peak powers of 65 kW. To our knowledge, these are the highest average powers obtained from cw, cw frequency-doubled and cw mode-locked Cr:LiCAF lasers reported to date.

2. Experimental setup

Figure 1 (top) shows a schematic of the diode-pumped Cr:LiCAF laser cavity used in cw laser experiments. Four linearly-polarized 1.8-W single-emitter multi-mode diodes (MMD-1 to MMD-4) from n-Light Photonics were used for pumping at a central wavelength of 665 nm. Each single emitter has a transverse area of 1 μm × 150 μm and contains built-in cylindrical microlenses to collimate the beam along the fast axis (perpendicular to the plane of the junction). The transverse pump characteristics were diffraction-limited along the fast axis and multimode along the slow axis with an M^2 value of approximately 10. Therefore, the output of the multimode diode lasers was first collected and collimated with an aspheric lens of a focal length of f = 4.5 mm and a numerical aperture of 0.54. Two of the diodes (MMD1-MMD3) were combined with polarization multiplexing, using a polarizing beam splitter cube (PBS) to

#233863 - $15.00 USD Received 3 Feb 2015; revised 10 Mar 2015; accepted 10 Mar 2015; published 30 Mar 2015

pump the crystal from one side. For pumping from the other direction, the output of MMD-2 and MMD-4 was combined in a similar manner. After passing through the PBS cubes, the pump modes were focused inside the laser crystal to a spot size of 25 μm × 70 μm using 100 mm focal length achromatic doublets. Inside the crystal, due to the Brewster cut surface, the pump spot size elongates in the horizontal direction and a spot size of 25 μm × 100 μm was formed.

In the cw laser experiments, astigmatically compensated X cavities with two curved pump mirrors (M1 and M2, R = 75 mm), a flat end mirror (M3) and output coupler (OC) were employed. Short and long cavity arm lengths were 25 cm and 30 cm, respectively. A cavity mode size of 25 μm × 35 μm was obtained inside the crystal. A 4-mm-long, 5% Cr-doped Cr:LiCAF crystal was used in these studies. The crystal absorbed more than 95% of the 660 nm pump light for both TE and TM polarizations. Due to reflection losses in pump optics and Fresnel losses from the crystals surface for TE polarized pump light, only 5.5 W of excitation power were absorbed by the crystal at the maximum pump output available of 7.2 W. The crystal was 1.5 mm thick and mounted with indium foil in a copper holder under water cooling. The laser performance was investigated using 3 different output couplers with transmission grades of 0.75%, 1% and 2% centered around 800 nm. The variation of laser power with crystal base temperature was also investigated. While cooling the mount to 3 °C resulted in an increase of output power between 10% and 20%, the temperature was kept at 10 °C to avoid water condensation at the end facets. A vertical slit near the output coupler enabled control of the output transverse mode.

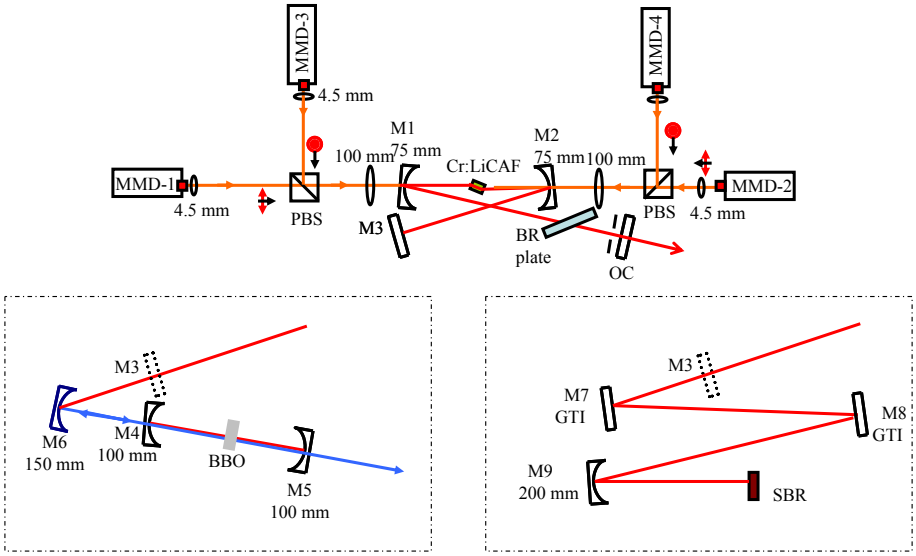

Fig. 1. Experimental setup of the multi-mode diode (MMD) pumped Cr:LiCAF laser. The schematic on the top describes the cw laser cavity. The flat high reflector (M3) was removed extending the cw cavity either for (i) intracavity frequency doubling (left) or for (ii) mode-locking experiments (right). PBS: polarizing beam splitter cube, OC: output coupler, BR plate: birefringent tuning plate, SBR: saturable Bragg reflector, GTI: Gires-Tournois interferometer.

For intracavity frequency doubling, the cavity was extended after removal of the flat high-reflector M3. The laser OC was also replaced by a flat high-reflector to boost intracavity power levels and improve nonlinear conversion efficiency. Two curved highly reflective mirrors with a radius of curvature of 100 mm (M4 and M5) have been inserted to generate a second focus [Fig. 1 (left)]. A 2-mm long flat-flat cut BBO crystal that was optimized for second-harmonic generation at 800 nm has been placed at this position. The BBO crystal had antireflection coatings both at the fundamental and second-harmonic wavelength regions. Curved mirrors M4 and M5 have a transmission of around 90% around 400 nm, acting as output couplers at the harmonic wavelength. To obtain a single output, the blue power

#233863 - $15.00 USD Received 3 Feb 2015; revised 10 Mar 2015; accepted 10 Mar 2015; published 30 Mar 2015

transmitted from M4 is retro-reflected back using a 150 mm radius of curvature metallic high reflector. A birefringent (BR) plate was inserted inside the cavity for wavelength tuning of the fundamental and harmonic emissions. This component also stabilized the blue output power by preventing shifts in laser wavelength.

In mode-locking experiments [Fig. 1 (right)] two Gires-Tournois interferometers (GTI, M7-M8) with a group velocity dispersion (GVD) of −550 ± 50 fs^2 per bounce in the range between 790 nm and 815 nm were used. The Cr^{3+}:LiCAF crystal with its GVD of + 25 fs^2/mm and the intra-cavity air path summed up to a dispersion of approximately + 250 fs^2. The BR tuning plate was removed from the cavity during the mode-locking experiments and the other optical elements inside the cavity had negligible dispersion around 800 nm. Therefore, we estimate a total round-trip cavity dispersion between −1750 to −2000 fs^2. To initiate and sustain mode locking, an 800 nm saturable Bragg reflector (SBR) with a modulation depth of 1% was used. A 200 mm radius of curvature mirror was employed to focus the intracavity mode onto the SBR surface to a spot size of 50 μm.

3. Experimental results

Figure 2 (left) shows the measured cw performance of the Cr:LiCAF laser. The free-running cw output wavelength was around 800 nm. The best cw result was obtained with the 2% output coupler. Using this component, the system produced up to 2540 mW of output power with 5470 mW of absorbed pump. The corresponding threshold and the slope efficiency with respect to absorbed pump power were 180 mW and 49%, respectively. In earlier work, slope efficiencies of 54% with single-mode diodes [20], 41% with tapered diodes [21], and 32% with multimode diodes [20] have been reported. The slope efficiency in the current work (49%) approaches the efficiencies obtained with single-mode diode pumping. Compared to earlier multimode diode pumped Cr:LiCAF laser results [20], efficiencies obtained in this study are significantly better. We believe this is enabled by (i) the lower chromium doping of the crystal (5% Cr-doped 4 mm crystal compared to 10% Cr-doped 2 mm long crystal in [20]) which facilitated better thermal management, and (ii) lower amount of passive losses inside the crystal (0.1% in this study versus 0.3% in [20]). The improved efficiencies in this work also allowed scaling of cw output powers from 1-W level to 2.54 W. Using the BR tuning plate, the laser could be tuned continuously from 745 nm to 885 nm with the 0.75% output coupler. The optical-to-optical conversion efficiency of the system was above 35%.

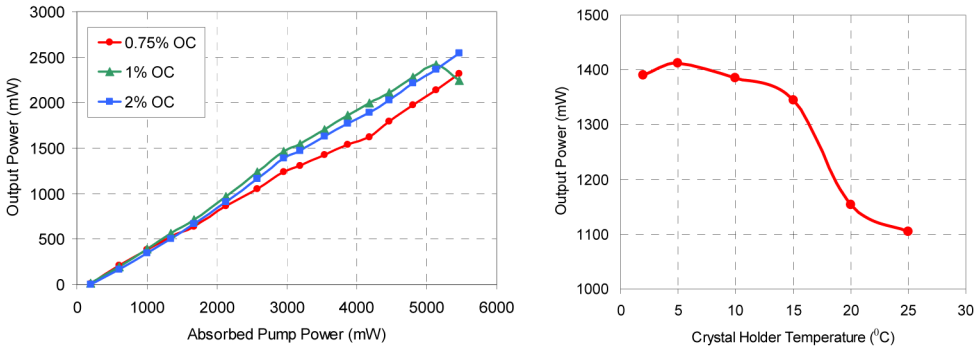

Fig. 2. (Left) Measured variation of the cw Cr:LiCAF laser power as a function of absorbed pump power for output couplers with transmissions of 0.75%, 1% and 2%, respectively. The data is taken at a crystal mount temperature of 10 °C. (Right) Measured variation of the cw Cr:LiCAF laser power as a function of crystal base temperature at an absorbed pump power of 2.3 W.

Figure 2 (right) shows the measured variation of cw laser performance with crystal holder temperature taken with the 2% output coupler at an absorbed pump power of 2.3 W. Note that a sharp decrease in laser power has been observed above a critical temperature of 15 °C. This finding indicates that the local temperature in some part of the Cr:LiCAF crystal reaches more

#233863 - $15.00 USD Received 3 Feb 2015; revised 10 Mar 2015; accepted 10 Mar 2015; published 30 Mar 2015

than 200 °C, representing a critical threshold for lifetime quenching [16]. The decrease in the upper state lifetime limits the output power by increasing the laser threshold. In our experiments, we have kept the crystal holder temperature at 10 °C to keep the thermal effects at a reasonable level.

Unfortunately, during our experiments we have observed cracking inside the Cr:LiCAF crystal while pumping with 6 W of incident power. We assign this effect to the thermal stress induced by the large anisotropy of the thermal expansion coefficient in LiCAF (thermal expansion coefficient is 22×10^{-6} and $3.6 \times 10^{-6}\,^{\circ}C^{-1}$ for E_|_c and E//c, respectively, where E is the electric field of the laser beam within the Brewster-cut crystal) [22–24]. Since lasing was blocked during the damage, we conclude that care must be taken to ensure efficient power extraction by stimulated emission when working in extreme regimes of pumping. On the other hand, even while the laser is operating regularly, there is considerable thermal load on the crystal. For example, for a laser that is operating with 50% slope efficiency, around half of the pump power is converted into heat. Hence, our experiments indicate that a pump power of approximately 2 × 6 W = 12 W is sufficient to initiate fracture in the 4-mm long, 5% Cr-doped Cr:LiCAF sample that was used in this study. In theory, one can use longer samples with lower chromium concentration and lower thermal load per unit length to increase the critical power for fracturing. On the contrary, the passive losses might increase with crystal length which can then limit the obtainable laser efficiencies and output powers. In any case, we believe that, for Cr: Colquiriites, obtaining cw output powers above 5 W is a very challenging engineering problem due to the inherent material limitations.

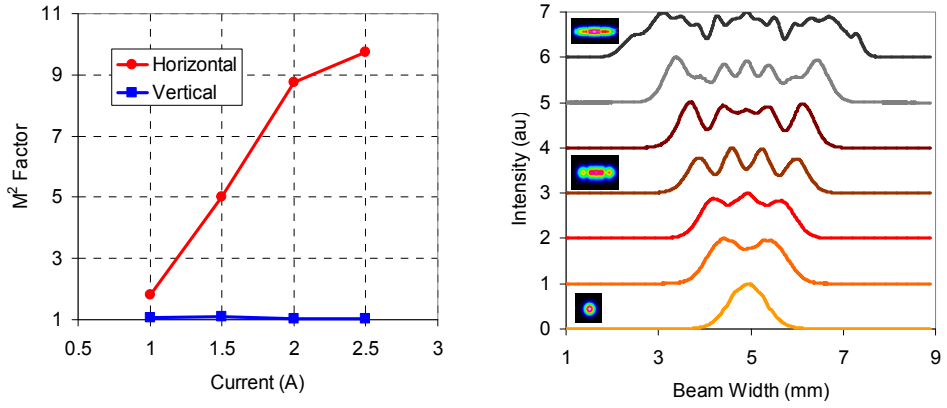

Fig. 3. (Left) Measured variation of the cw Cr:LiCAF laser output beam quality (M^2 factor) as a function of diode supply current. (Right) Variation of Cr:LiCAF laser output beam profile in the horizontal/slow axis as a function of diode current. The insets show recorded transverse beam profiles.

Figure 3 (left) shows the measured variation of cw laser output beam quality (M^2 factor) in the horizontal and vertical axis as a function of diode current. Here the horizontal and vertical axes correspond to slow and fast axes of the diode, respectively. As mentioned earlier, at the full MMD current (2.5 A), the diodes have an M^2 of 1.1 and 10 in the fast and slow axes, respectively. As we can see from Fig. 4, the Cr:LiCAF laser output closely follows the properties of the pump beam, reaching identical beam quality at the full pump power. As the pump current is decreased, the pump beam quality in the horizontal/fast axis improves as well as the one of Cr:LiCAF laser [Fig. 3(b)]. Lastly, a slit near the OC (tangential plane) could also be used to control the transverse mode structure of the laser output. With the slit width adjusted properly, it was possible to obtain a symmetric diffraction limited TEM_{00} laser beam at the expense of decreased levels of output power (1.1 W for the TEM_{00} output).

#233863 - $15.00 USD Received 3 Feb 2015; revised 10 Mar 2015; accepted 10 Mar 2015; published 30 Mar 2015

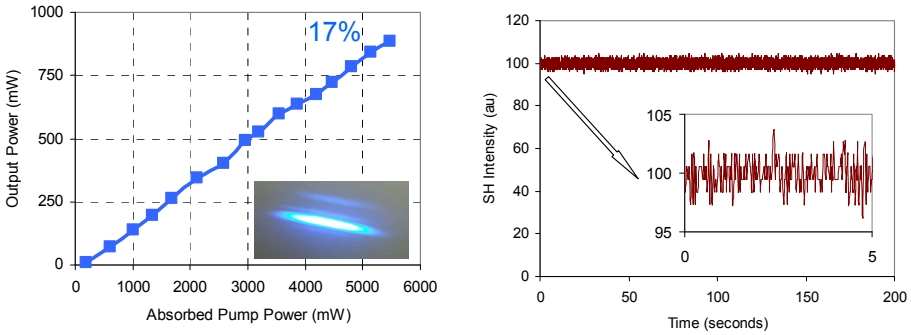

Fig. 4. (Left) Measured variation of the intracavity-generated cw blue output as a function of absorbed pump power. Inset figure shows a picture of the output beam. (Right) Measured variation of blue intensity with time. Inset figure is a zoomed-in version which shows the first 5 seconds.

Figure 4 (left) shows the measured blue power levels as a function of absorbed pump. At the maximum excitation level of 5.5 W, up to 900 mW of cw second-harmonic power have been generated at a central wavelength of 400 nm. We have not used the intracavity slit during these experiments, and the blue output was multimode. The optical-to-optical conversion efficiency of the system was 12.5% and 16.5% with respect to incident and absorbed pump power levels, respectively. To our knowledge, these are the highest cw frequency-doubled laser powers and conversion efficiencies obtained from Cr:Colquiriites to date [25]. On the other hand, according to the theory of intracavity second-harmonic generation, maximum frequency-doubled powers could be as high as the maximum available fundamental output from the laser [26]. Hence, further improvement of nonlinear crystal geometry, coating and focusing, second harmonic powers may be scaled above 2 W. Figure 4 (right) shows the measured fluctuations in the generated second harmonic intensity. Note that the second-harmonic intensity is quite stable with a relative standard deviation less than 1.5%. Also, the BR plate enabled continuous tuning of the blue output from 375 nm to 440 nm. Measured frequency doubled output powers were above 500 mW for wavelengths between 385 nm and 415 nm. Outside this region, second harmonic conversion efficiency decreased sharply due to the non-optimum performance of the 800 nm frequency doubling crystal (non-optimum AR coating and cut angle). However, by using nonlinear crystals that are optimized around 750 nm and 850 nm, one can improve the frequency-doubled output powers also at the edges of the tuning range. Lastly, a similar intracavity conversion scheme with an optical parametric oscillator may be used to extend the wavelength range further into the near infrared [27].

In mode locking experiments, various dispersion settings, output couplers and focusing geometries on the SBR were studied to optimize performance. Cr:LiCAF is a low-gain medium with a relatively small emission cross section, rendering it quite susceptible to Q-switched mode-locking. Therefore, SBR position, dispersion and output coupling may be carefully adjusted to obtain clean cw mode-locking with suppressed tendency for Q-switching. Although pulses as short as 40 fs might be obtained with SBR mode-locked Cr:LiCAF, we have focused our attention on maximization of average power and for this end it was easier to work with 100-fs level pulses in our experiments.

Figure 5(a) shows the variation of laser output power and laser dynamics with absorbed pump power under 2% output coupling. The laser operated in cw mode for absorbed pump powers up to 3.5 W and generated Q-switched mode-locked pulses for pump powers between 4 W and 4.5 W (QS-ML). Stable cw mode-locking (cw ML) was obtained above 5 W of pump power. The optical spectrum, an autocorrelation trace and the microwave spectrum taken with the 2% output coupler at a pump power of 5.5 W are depicted in Fig. 5(b)-5(d). The laser produced 105-fs pulses (assuming sech^2 pulses) with 750 mW of average power and

#233863 - $15.00 USD Received 3 Feb 2015; revised 10 Mar 2015; accepted 10 Mar 2015; published 30 Mar 2015

6 nm spectral bandwidth near 810 nm at 96.4 MHz repetition rate, corresponding to a pulse energy of 7.7 nJ and peak power of 65 kW. The optical spectrum was modulated due to spectral oscillations of dispersion (mostly from the GTI mirror) and perturbations of solitonic pulse propagation resulting in Kelly side bands. The time-bandwidth product was 0.4, slightly above the transform limit of 0.315 for $sech^2$ pulses. For cw mode-locked operation, the optical-to-optical conversion efficiency of the system was above 10% (750 mW / 7.2 W). The laser output was slightly multimode with an M^2 of about 2 in the horizontal/slow axis (some of the higher order lateral modes were eliminated due to the additional losses from the SBR). With the intracavity slit width adjusted, a TEM_{00} laser output mode could also be obtained with output powers around 500 mW. To our knowledge, these results represent the highest average and peak powers, as well as maximum pulse energies obtained to date from femtosecond Cr^{3+}:colquiriite oscillators at standard repetition rates. Note that pulse energies and peak powers may be further scaled using multi-pass cavities [28] or cavity dumping.

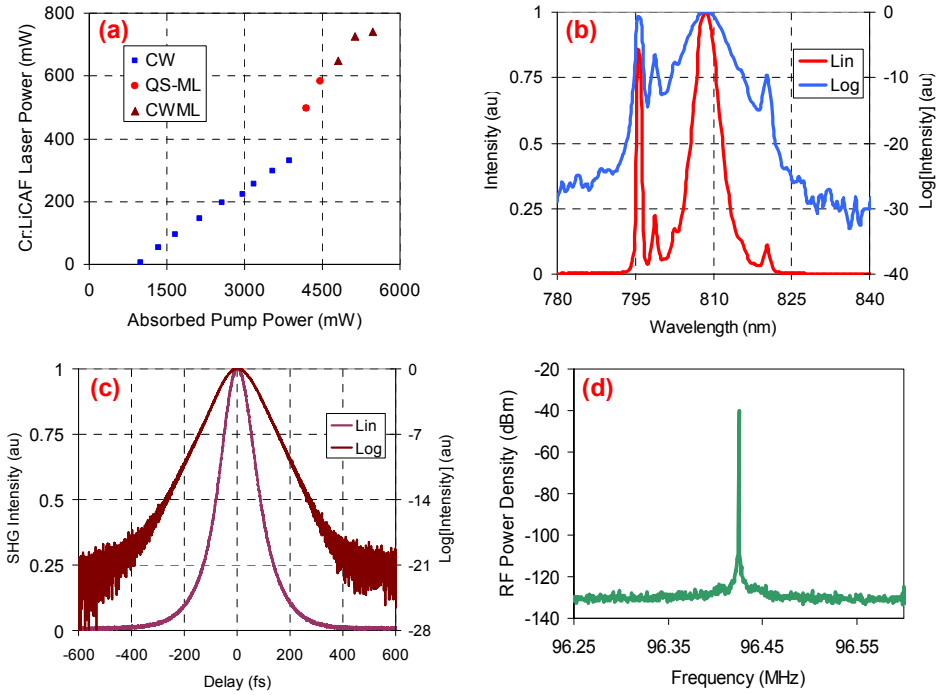

Fig. 5. Continuous-wave mode-locking results: (a) Laser efficiency of the multimode diode pumped mode-locked Cr:LiCAF laser in different regimes of operation taken with the 2% output coupler. CW: continuous-wave operation, QS-ML: Q-switched mode-locked operation, CWML: continuous-wave mode-locked operation. Measured optical spectrum (b), autocorrelation (c), and radio frequency spectrum (d) for the 105-fs long pulses with 750 mW of average power and 96.4 MHz repetition rate.

Another potential way of scaling pulse energies in Cr:LiCAF lasers is exploring the Q-switched mode-locked (QS-ML) regime. In this scheme, the laser produces femtosecond pulses under a Q-switched intensity envelope. Figure 6(a) shows the typical QS-ML pulse train obtained from the multimode diode pumped Cr:LiCAF laser. Q-switched mode-locked operation with average powers as high as 1625 mW have been obtained at a pump power of 5.5 W [Fig. 6(b)]. Mode-locked and Q-switched repetition rates were 143.5 MHz and 33 kHz, respectively [Fig. 6(d)]. Each Q-switched pulse envelope has a width of approximately 2 microseconds and carries a total energy of 2 μJ. The period of time between individual femtosecond pulses is 6.97 ns. Each Q-switched envelope contains about 600 pulses. The peak pulse energies within the Q-switched envelope are above 150 nJ. The optical spectrum

#233863 - $15.00 USD Received 3 Feb 2015; revised 10 Mar 2015; accepted 10 Mar 2015; published 30 Mar 2015

of the pulses is centered around 794.5 nm with a FWHM of 2.75 nm [Fig. 6(c)], supporting 250-fs long pulses. Consequently, the corresponding peak power exceeds 500 kW. We believe that the QS-ML Cr:LiCAF laser might be useful for applications such as deep-tissue multiphoton microscopy [29, 30] or three dimensional micromachining of photonics devices [31] where pulse to pulse fluctuations in energy and peak power are not critical.

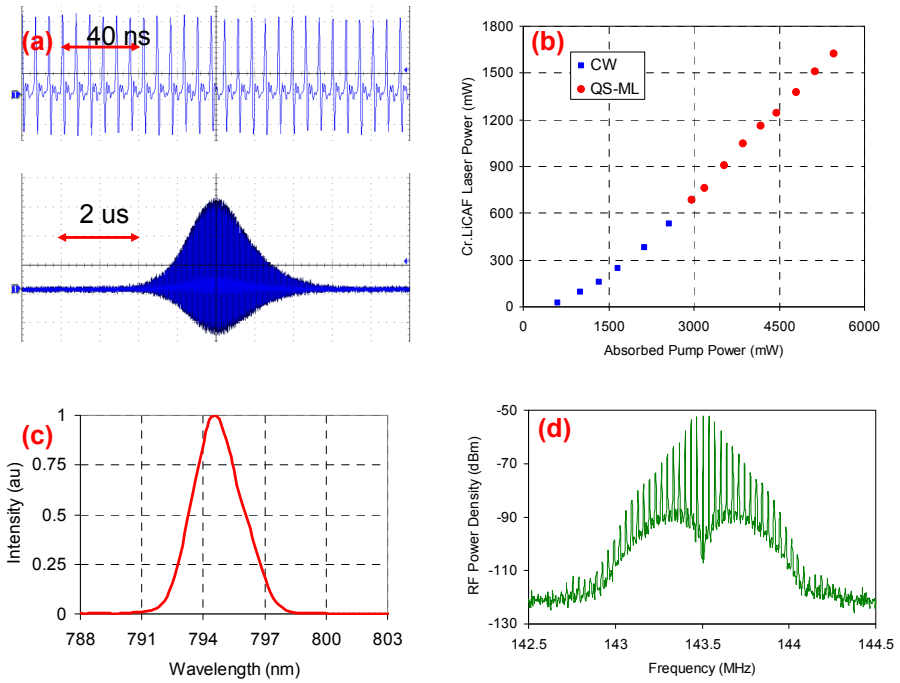

Fig. 6. Q-switched mode-locking results: (a) Q-switched pulse train intensity versus time, (b) laser efficiency of the mode-locked Cr:LiCAF laser in different regimes of operation taken with the 2% output coupler. Measured optical (c) and radio frequency spectra (d).

5. Conclusions

In summary, we have demonstrated multi-mode diode pumped cw, cw frequency-doubled and cw mode-locked Cr:LiCAF lasers operating with record efficiencies and power levels. CW output as high as 2.54 W around 800 nm, frequency-doubled blue emission up to 900 mW around 400 nm and cw mode-locked average powers of 750 mW at a pulse duration of 105 fs have been demonstrated. Fundamental and frequency-doubled laser output was tuned continuously in a broad wavelength range between 745 nm and 885 nm as well as from 375 nm to 440 nm, respectively, applying an intracavity birefringent plate. We have experienced cracking of the Cr:LiCAF crystal induced by thermal stress under 6 W of pump power. This finding indicates that the large anisotropy of thermal conductivity of Cr:LiCAF might pose severe challenges to further power scaling. Finally, individual pulse energies higher than 150 nJ have been reached when mode-locked operation was combined with Q-switching.

Acknowledgments

We acknowledge financial support from TUBITAK (The Scientific and Technological Research Council of Turkey, 112T220), European Union Marie Curie Career Integration Grant (PCIG11-GA-2012-321787), Center for Applied Photonics of Konstanz University and Alexander von Humboldt-Foundation.